also able to transport fluconazole, was used as a counter-screen that allowed us to select for specific inhibitors of ABC transporters [5].

UnmA and UnmC were originally isolated as compounds exhibiting antibacterial activity [12]. In the agar diffusion assay disks containing 13 nmol of UnmA and UnmC gave significant growth inhibitory zones when the AD/CaCDR1 cells were co-exposed to sub-MIC concentrations of fluconazole (Fig. 2). This inhibitory activity of UnmA and UnmC was specific for AD/CaCDR1 cells, as these compounds did not affect the growth of AD/CaCDR2 or AD/CaMDR1 cells at comparable levels of sub-MIC concentrations of fluconazole (Fig. 2). UnmA and UnmC gave growth inhibitory zones of AD/CaCDR1 cells in the presence of sub-MIC concentrations of fluconazole that were comparable to FK506. FK506 has been reported to be an inhibitor of some ABC transporters and was therefore able to chemosensitize cells that were overexpressing these multi-drug efflux pumps [2]. UnmA and UnmC alone did not inhibit the growth of the parental control strain AD/pABC3 (Fig. 2), nor AD/CaCDR1 or AD/CaMDR1 cells (data not shown). To test whether UnmA and UnmC are able to inhibit a broader range of fungal multi-drug efflux pumps yeast cells overexpressing the highly homologous multi-drug efflux pumps from *Candida glabrata* CgCdr1p, CgPdh1p and *S. cerevisiae* ScPdr5p, as well as two fluconazole-resistant *C. albicans* clinical isolates were tested for their ability to be chemosensitized to fluconazole by UnmA and UnmC as well as FK506. Growth of strains expressing *C. glabrata* ABC transporters CgCdr1p and CgPdh1p was dramatically inhibited in the presence of sub-MIC concentrations of fluconazole by any of these three compounds. A similarly large growth inhibitory effect of FK506 was detected for ScPdr5p overexpressing cells. The sizes of inhibitory zones produced by UnmA and UnmC compared to FK506 were slightly smaller for CaCdr1p and ScPdr5p overexpressing strains and the *C. albicans* clinical isolate B59630 but significantly larger for the *C. albicans* clinical isolate CaAD (Fig. 2). The two clinical isolates overexpress both CaCdr1p and CaCdr2p and are highly resistant to antifungal drugs including fluconazole and ketoconazole [13]. Our results suggest that both UnmA and UnmC inhibit the fluconazole transport of a variety of fungal multi-drug efflux pumps including *C. glabrata* CgCdr1p and CgPdh1p, *C. albicans* CaCdr1p and *S. cerevisiae* ScPdr5p overexpressed in *S. cerevisiae* and, more significantly, inhibit the homologously overexpressed *C. albicans* CaCdr1p transporter in resistant clinical *C. albicans* isolates.

Chemosensitization of S. cerevisiae strains overexpressing C. albicans drug efflux pumps and chemosensitization of azole-resistant C. albicans clinical isolates to fluconazole

A quantitative chemosensitization (checkerboard) assay was performed to evaluate the synergistic effects of UnmA and UnmC on the growth of *C. albicans* drug efflux pump overexpressing *S. cerevisiae* strains in the presence of varying amounts of fluconazole. The MIC of fluconazole with AD/CaCDR1 (320 μg/ml) was reduced to 5 μg/ml when 10 μM UnmA or 1.25 μM UnmC was present (Table 2). In contrast, the presence of UnmA and UnmC did not change the MICs of fluconazole of AD/CaCDR2 and AD/CaMDR1. The FIC indices of FK506, UnmA, and UnmC with fluconazole for the growth inhibition of AD/CaCDR1 cells were 0.266, 0.141, and 0.031, respectively (Table 2). The FIC indices indicated that UnmA and UnmC chemosensitized AD/CaCDR1 cells to fluconazole more effectively than FK506. No synergy between fluconazole and these inhibitors was detected for AD/CaCDR2 yeast cells, with the FIC indices being two for both UnmA and UnmC (Table 2).

The chemosensitization assay to fluconazole was also performed with two *C. albicans* clinical isolates CaAD [14] and B59630 [15] (Table 2). Both UnmA and UnmC chemosensitized these azole resistant *C. albicans* clinical isolates to fluconazole as effectively as AD/CaCDR1 cells. This result suggests that both UnmA and UnmC could potentially be used as an adjuvant to help attenuate azole resistance of clinical *C. albicans* isolates.

UnmA and UnmC inhibit the efflux of R6G and the ATPase activity of CaCdr1p overexpressing yeast cells

The fluorescent compound R6G is a known substrate of many ABC transporters including CaCdr1p and CaCdr2p

Table 2
Chemosensitization of *S. cerevisiae* AD1-8u$^-$ strains overexpressing *C. albicans* efflux pumps and fluconazole-resistant *C. albicans* clinical isolates to fluconazole by FK506, unnarmicin A or unnarmicin C

Strain	MIC of fluconazole alone[a]	FK506			Unnarmicin A			Unnarmicin C		
		MIC^{Fb}	MIC^{Ic}	FIC	MIC^{Fb}	MIC^{Ic}	FIC	MIC^{Fb}	MIC^{Ic}	FIC
AD/CaCDR1	320	5 (40)	160	0.266	5 (10)	80	0.141	5 (1.25)	80	0.031
AD/CaCDR2	80	80 (80)	80	2	80 (160)	160	2	80 (160)	160	2
AD/CaMDR1	40	10 (10)	160	0.313	40 (80)	80	2	40 (160)	160	2
CaAD	40–80	20 (1.25)	320	0.254	10 (0.312)	320	0.251	10 (0.312)	320	0.251
B59630	320	20 (20)	320	0.281	40 (1.25)	320	0.129	40 (5)	320	0.141

[a] MIC (μg/ml) of fluconazole was determined with CSM-URA medium.
[b] MIC (μg/ml) of fluconazole in combination with inhibitors at an indicated concentration (μM) in parentheses.
[c] MIC (μM) of inhibitor alone.

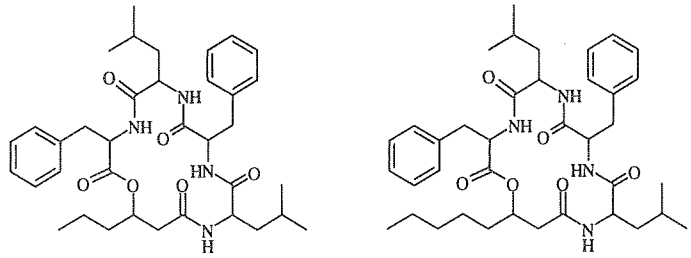

unnarmicin A unnarmicin C

Fig. 1. Structures of unnarmicin A and unnarmicin C.

and is often used to measure the drug efflux from cells overexpressing these pumps [3,16]. The effects of UnmA and UnmC on the glucose-dependent R6G efflux were assayed as described in Materials and methods. At a concentration of 20 μM, both UnmA and UnmC strongly inhibited (80%) the R6G efflux of CaCdr1p but had no inhibitory effect at all on CaCdr2p (Fig. 3). UnmA and UnmC gave comparable IC_{50} values of 3.61 ± 1.05 and 5.65 ± 1.96 μM, respectively. These results suggest that both UnmA and UnmC directly inhibit the transport activity of CaCdr1p.

The ATPase activity of ABC transporters is required for the active transport of pump substrates [17]. The effects of UnmA and UnmC on the vanadate sensitive ATPase activities of ABC transporters were tested using purified plasma membrane fractions. The ATPase activity of CaCdr1p was inhibited by either UnmA or UnmC at IC_{50} values of 0.495 ± 0.225 and 0.688 ± 0.243 μM, respectively (Fig. 4). And as expected, the ATPase activity of CaCdr2p was not affected by these compounds.

Discussion

Overexpression of ABC transporters confers highest levels of multi-drug resistance of pathogenic fungi. One strategy aimed at suppressing this most clinically significant form of multi-drug resistance in pathogenic fungi is to develop specific inhibitors of fungal ABC transporters. The inhibition of drug efflux pumps will allow the antifungal drug to accumulate at toxic levels inside the cell and inhibit fungal growth. We have obtained new inhibitors of fungal multi-drug transporters by screening a series of compounds and crude extracts from marine-derived fungi and bacteria. Two structurally related cyclic peptides, UnmA and UnmC, were found to inhibit the clinically significant fungal ABC transporters CaCdr1p and CgCdr1p.

UnmA and UnmC are cyclodepsipeptides consisting of four amino acids and a 3-hydroxy fatty acid. They only differ in the length of the alkyl chain of the fatty acid (Fig. 1). Combining UnmA and UnmC with fluconazole in a checkerboard assay gave slightly enhanced growth inhibition for UnmC compared with UnmA (Table 2) while UnmA gave more extensive chemosensitization in agar diffusion assays. However, UnmA and UnmC inhibited the R6G efflux from AD/CaCDR1 cells at very similar IC_{50} values. The ATPase activity of CaCdr1p that drives the active drug transport was also inhibited to a similar extent by both UnmA and UnmC, but at 10-fold lower IC_{50} values of UnmA and UnmC than were needed to inhibit the R6G efflux. These data suggest that the length of the alkyl side chain may significantly affect the different efficacies of these two compounds when using different biochemical assays but from the *in vitro* ATPase assays it appears that both compounds have similar affinities to their target proteins and therefore inhibitory activities. The 10-fold lower concentration of

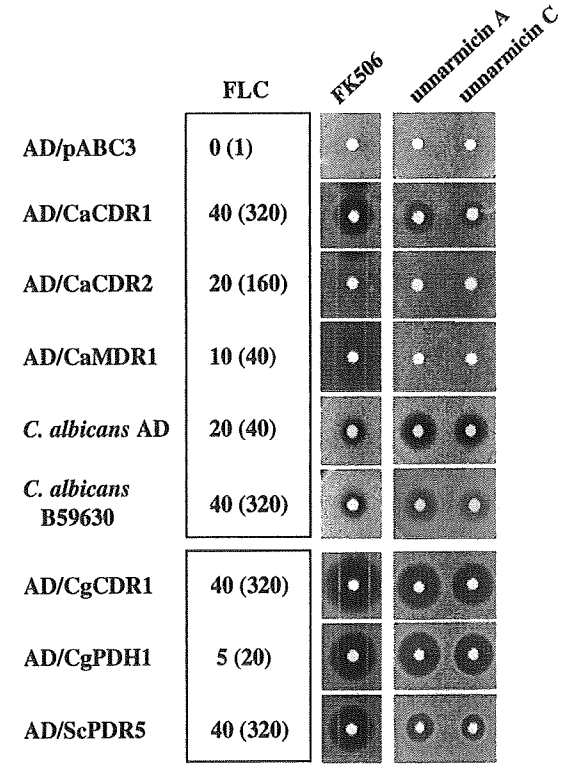

Fig. 2. Chemosensitization of efflux pump expressing strains of *S. cerevisiae* and of fluconazole-resistant *C. albicans* clinical isolates to fluconazole with specific pump inhibitors. Inhibitors were placed on disks on YPD agar plates containing sub-MIC (μg/ml) concentrations of fluconazole as indicated in the fluconazole (FLC) column. Numbers in parentheses indicate MIC of fluconazole of each strain. FK506 (12 nmol/disk), unnarmicin A, and unnarmicin C (13 nmol/disk, each) were loaded onto disks and plates containing a lawn of the indicated strains incubated at 30 °C for 24 h.

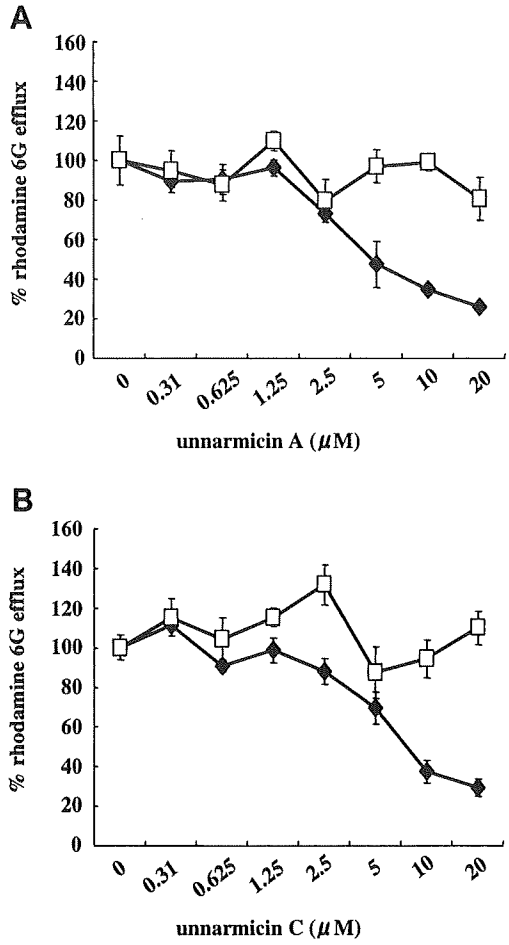

Fig. 3. Rhodamine 6G efflux assay of pump overexpressing strains. AD/CaCDR1 and AD/CaCDR2 cells were starved with 2-deoxy glucose to allow the uptake of R6G and washed. Addition of glucose initiated the efflux of R6G from cells. The released R6G was quantified using a fluorescent microplate reader. Filled square, AD/CaCDR1; open square, AD/CaCDR2. (A) Inhibition curve for unnarmicin A, (B) inhibition curve for unnarmicin C.

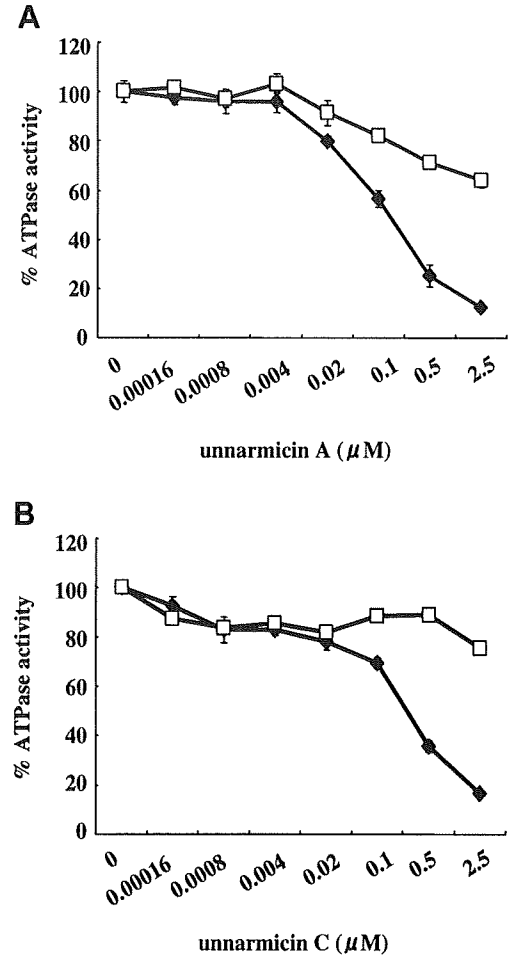

Fig. 4. ATPase assay of plasma membrane fractions isolated from pump expressing strains. Plasma membrane fractions were isolated from AD/pABC3 (vector), AD/CaCDR1, and AD/CaCDR2 cells harvested at stationary phase. Membranes were incubated with ATP and inhibitors, and released P_i was measured as described in Materials and methods. ATPase activities of either CaCdr1p or CaCdr2p in the presence of inhibitors are represented as a percentage of the ATPase activity in the absence of inhibitor. Filled square, AD/CaCDR1; open square, AD/CaCDR2. (A) Inhibition curve for unnarmicin A, (B) inhibition curve for unnarmicin C.

UnmA and UnmC required to specifically inhibit the ATPase activity of CaCdr1p, but not CaCdr2p, compared to the levels required to inhibit the R6G efflux of whole cells leads us to speculate that the site of inhibition may lie at the cytoplasmic face of the protein that is only directly accessible in the *in vitro* ATPase assay.

FK506 and enniatins were reported to inhibit fungal ABC transporters, but they have severe toxicity against yeasts under some conditions such as high pH or when grown in nutrient-poor synthetic medium (unpublished data) [18]. FK506 did not chemosensitize AD/CaMDR1 cells to fluconazole in a disk diffusion assay using YPD agar plates (Fig. 2) but it slightly chemosensitized these cells in a checkerboard assay using CSM-URA medium through some unknown mechanism that is possibly associated with its known inhibitory effect of the calcineurin pathway which is important for yeast cells to be able to respond to a range of environmental stresses (Table 2) [5]. UnmA and UnmC were less toxic to *S. cerevisiae* and *C. albicans* cells than FK506 (data not shown), and did not affect the growth of AD/CaMDR1 cells, indicating that in contrast to FK506 these two compounds appear to have no other potential target sites inside yeast cells at the tested concentration range. Despite their antibacterial activity, UnmA and UnmC might therefore be harmless for the commensal fungal flora.

Neither UnmA nor UnmC inhibited the growth of AD/CaCDR2 in the presence of fluconazole, however, CaCdr1p and CaCdr2p display extensive sequence homology with each other (84% identity and 92% similarity) [19]. The amino acid sequence differences between CaCdr1p and CaCdr2p are distributed throughout the molecules but are mainly found in both transmembrane domains (TMDs). This also supports the idea that the site of inhibi-

tion of UnmA and UnmC lies more likely within the TMDs which are also more readily accessible in the *in vitro* ATPase assay. This could also explain why 10-fold lower concentrations of both UnmA and UnmC are needed to inhibit the *in vitro* ATPase activity compared to the levels needed to inhibit the *in vivo* efflux of R6G using whole cells. We observed that UnmA and UnmC, both specific inhibitors of CaCdr1p, could fully inhibit the growth of clinically resistant *C. albicans* isolates in combination with fluconazole (Fig. 2 and Table 2). The expression of both CaCdr1p and CaCdr2p is frequently upregulated in azole resistant clinical isolates [1]. Our results therefore support the idea that CaCdr1p makes a greater contribution than CaCdr2p to azole resistance in clinical isolates [20].

In this study, we found compounds from marine gammaproteobacterium that specifically inhibit some fungal ABC transporters. These new inhibitors may also be useful in investigating molecular mechanisms of ABC transporters.

Acknowledgments

We gratefully acknowledge financial support from the Health and Labour Sciences Research Grants for Research on Emerging and Re-emerging Infectious Diseases, Japan's Ministry of Health, Labour and Welfare (awarded to Y.U. (H16-Shinko-034)) and the Japan Health Sciences Foundation (awarded to K.T. (KH33310) and M.N. (SH244405)). The authors thank B.C. Monk for critical reading of the manuscript and Astellas Pharma Inc. for providing FK506.

References

[1] T.C. White, K.A. Marr, R.A. Bowden, Clinical, cellular, and molecular factors that contribute to antifungal drug resistance, Clin. Microbiol. Rev. 11 (1998) 382–402.

[2] S. Maesaki, P. Marichal, M.A. Hossain, D. Sanglard, H. Vanden Bossche, S. Kohno, Synergic effects of tacrolimus and azole antifungal agents against azole-resistant *Candida albicans* strains, J. Antimicrob. Chemother. 42 (1998) 747–753.

[3] K. Hiraga, S. Yamamoto, H. Fukuda, N. Hamanaka, K. Oda, Enniatin has a new function as an inhibitor of Pdr5p, one of the ABC transporters in *Saccharomyces cerevisiae*, Biochem. Biophys. Res. Commun. 328 (2005) 1119–1125.

[4] M.D. Lee, J.L. Galazzo, A.L. Staley, J.C. Lee, M.S. Warren, H. Fuernkranz, S. Chamberland, O. Lomovskaya, G.H. Miller, Microbial fermentation-derived inhibitors of efflux-pump-mediated drug resistance, Il Farmaco 56 (2001) 81–85.

[5] E. Lamping, B.C. Monk, K. Niimi, A.R. Holmes, S. Tsao, K. Tanabe, M. Niimi, Y. Uehara, R.D. Cannon, Characterization of three classes of membrane proteins involved in fungal azole resistance by functional hyperexpression in *Saccharomyces cerevisiae*, Eukaryot. Cell 6 (2007) 1150–1165.

[6] K. Niimi, D.R. Harding, R. Parshot, A. King, D.J. Lun, A. Decottignies, M. Niimi, S. Lin, R.D. Cannon, A. Goffeau, B.C. Monk, Chemosensitization of fluconazole resistance in *Saccharomyces cerevisiae* and pathogenic fungi by a D-octapeptide derivative, Antimicrob. Agents Chemother. 48 (2004) 1256–1271.

[7] O. Marchetti, J.M. Entenza, D. Sanglard, J. Bille, M.P. Glauser, P. Moreillon, Fluconazole plus cyclosporine: a fungicidal combination effective against experimental endocarditis due to *Candida albicans*, Antimicrob. Agents Chemother. 44 (2000) 2932–2938.

[8] M. Niimi, S. Wada, K. Tanabe, A. Kaneko, Y. Takano, T. Umeyama, N. Hanaoka, Y. Uehara, E. Lamping, K. Niimi, S. Tsao, A.R. Holmes, B.C. Monk, R.D. Cannon, Functional analysis of fungal drug efflux transporters by heterologous expression in *Saccharomyces cerevisiae*, Jpn. J. Infect. Dis. 58 (2005) 1–7.

[9] B.C. Monk, R.D. Cannon, K. Nakamura, M. Niimi, K. Niimi, D.R.K. Harding, A.R. Holmes, E. Lamping, A. Goffeau, A. Decottignies, Membrane protein expression system and its application, International patent PCT/NZ02/00163, 2002.

[10] D.P. Kontoyiannis, R.E. Lewis, Combination chemotherapy for invasive fungal infections: what laboratory and clinical studies tell us so far, Drug Resist. Update 6 (2003) 257–269.

[11] S. Wada, M. Niimi, K. Niimi, A.R. Holmes, B.C. Monk, R.D. Cannon, Y. Uehara, *Candida glabrata* ATP-binding cassette transporters Cdr1p and Pdh1p expressed in a *Saccharomyces cerevisiae* strain deficient in membrane transporters show phosphorylation-dependent pumping properties, J. Biol. Chem. 277 (2002) 46809–46821.

[12] K. Adachi, K. Kawabata, H. Kasai, A. Katsuta, Y. Shizuri, Novel antibiotic cyclic peptides unnarmicins produced by *Photobacterium*, Jpn. Kokai Tokkyo Koho, JP 2007223969, 2007.

[13] G.D. Albertson, M. Niimi, R.D. Cannon, H.F. Jenkinson, Multiple efflux mechanisms are involved in *Candida albicans* fluconazole resistance, Antimicrob. Agents Chemother. 40 (1996) 2835–2841.

[14] F.C. Odds, Antifungal susceptibility testing of *Candida* spp. by relative growth measurement at single concentrations of antifungal agents, Antimicrob. Agents Chemother. 36 (1992).

[15] J.F. Ryley, R.G. Wilson, K.J. Barrett-Bee, Azole resistance in *Candida albicans*, Sabouraudia 22 (1984) 53–63.

[16] K. Nakamura, M. Niimi, K. Niimi, A.R. Holmes, J.E. Yates, A. Decottignies, B.C. Monk, A. Goffeau, R.D. Cannon, Functional expression of *Candida albicans* drug efflux pump Cdr1p in a *Saccharomyces cerevisiae* strain deficient in membrane transporters, Antimicrob. Agents Chemother. 45 (2001) 3366–3374.

[17] A.E. Senior, M.K. Al-Shawi, I.L. Urbatsch, The catalytic cycle of P-glycoprotein, FEBS Lett. 377 (1995) 285–289.

[18] C.S. Hemenway, J. Heitman, Lic4, a nuclear phosphoprotein that cooperates with calcineurin to regulate cation homeostasis in *Saccharomyces cerevisiae*, Mol. Gen. Genet. 261 (1999) 388–401.

[19] C. Gauthier, S. Weber, A.M. Alarco, O. Alqawi, R. Daoud, E. Georges, M. Raymond, Functional similarities and differences between *Candida albicans* Cdr1p and Cdr2p transporters, Antimicrob. Agents Chemother. 47 (2003) 1543–1554.

[20] D. Sanglard, F. Ischer, M. Monod, J. Bille, Susceptibilities of *Candida albicans* multidrug transporter mutants to various antifungal agents and other metabolic inhibitors, Antimicrob. Agents Chemother. 40 (1996) 2300–2305.

Jpn. J. Med. Mycol.
Vol. 50, 75 – 83, 2009
ISSN 0916 – 4804

Reviews

Application of *In Situ* Hybridization to Tissue Sections for Identification of Molds Causing Invasive Fungal Infection

Minoru Shinozaki[1], Yoichiro Okubo[1], Haruo Nakayama[1], Aki Mitsuda[1], Tadashi Ide[1], Somay Yamagata Murayama[2], Kazutoshi Shibuya*[1]

[1] Department of Surgical Pathology, Toho University School of Medicine
6-11-1 Omori-Nishi, Ota-Ku, Tokyo143-8541, Japan
[2] Laboratory of Molecular Epidemiology for Infectious Agents,
Graduate School of Infection Control Sciences & Kitasato Institute for Life Sciences
Kitasato University
5-9-1 Shirokane, Minato-ku, Tokyo 108-8641, Japan

Abstract

The present article describes our studies to know the usefulness of *in situ* hybridization (ISH) to identify various kinds of mold observed in tissue sections and/or cytological preparations from the lesions of patients with invasive fungal infection. To establish the precise procedure for ISH in formalin-fixed and paraffin-embedded sections, various pretreatments were attempted. The condition finally chosen is written here providing a favorable outcome regarding to both intensity and specificity of signals on outline of molds observed in the tissue sections when specimens were treated with both heat and proteinase K and, solutions were adjusted to higher pH value.

Therefore, usefulness of promising probes, two each DNA and peptide nucleic acid (PNA) were verified with a favorable pretreatment condition, using lungs of mice experimentally infected and/or those obtained from autopsies with invasive mold infection. As the result, DNA probes targeting alkaline proteinase (*ALP*) gene and retrotransposon *Afut*-1 gene of *Aspergillus fumigatus* showed specific signal intensity for the *Aspergillus* species and *A. fumigatus*, respectively. PNA probes for *Candida albicans* and the *Fusarium* species also showed satisfactory specificity. We wish to emphasize that ISH can be a valuable tool to identify medically important molds in formalin-fixed and paraffin-embedded tissue sections or cytological preparations.

Key words : *in situ* hybridization, *Aspergillus fumigatus*, histopathological diagnosis, invasive fungal infection, polymerase chain reaction (PCR)

Introduction

Histopathological and cytological examination has been regarded as one of the most important diagnostic tool for invasive fungal infections. It is essentially archived by detailed observation on shape of fungi demonstrated in paraffin-embedded tissue sections or alcohol-fixed cytological specimens. Although rapid and accurate diagnosis of invasive fungal infections becomes more important for successful antifungal therapy in contemporary medicine[1, 2], it is sometime difficult to identify the fungal species in the tissue specimens, especially in case of mold infection[3-5]. Therefore, it is required to establish a rapid and accurate method of diagnosis in pathological fields. Whereas sensitive and rapid molecular detection assays have been recently introduced by use of polymerase chain reaction (PCR) methods to detect *Aspergillus* DNA in serum, total blood[6-9], or tissue samples[10, 11], it is still hard to gain satisfactory specificity. On the other hand, there have been a few attempts to use *in situ* hybridization (ISH) to identify fungi in histopathological specimens[12-17]. To date, the study of ISH for diag-

Address for correspondence : Kazutoshi Shibuya
Department of Surgical Pathology, Toho University School of Medicine,
6-11-1, Omori-Nishi, Ota-Ku, Tokyo143-8541 Japan

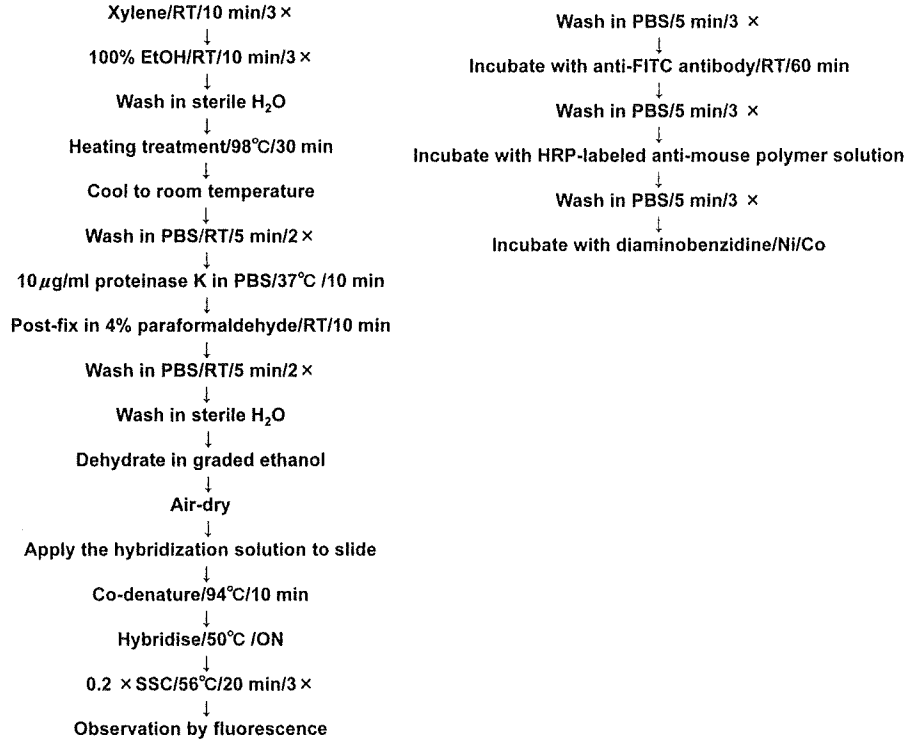

Fig. 1. Flow chart of *in situ* hybridization procedure in the present study.

nosis of fungal infection with formalin-fixed and paraffin-embedded sections has not been systematically promoted. This article deals with our attempts to detect fungus-specific nucleic acids in routinely prepared tissue sections by ISH.

1. Standard procedure of ISH

In the present study, the ISH was performed with following to the procedure shown in figure 1 as the flow chart (Fig. 1).

2. Design and preparation of probes

For the present study, we employed both double stranded DNA probes and peptide nucleic acid (PNA) probes among probes previously introduced. These probes were conjugated with fluorescein isothiocyanate (FITC). After observation of FISH preparations under fluorescent microscope, FITC indicating fungi on the sections was immunohistochemically transferred to the peroxidase end product with treatment of anti-FITC antibody and horseradish peroxidase-labeled polymer solution.

Since the genes encoding virulence factors of various fungi can be used for the marker of molecular diagnosis, DNA targeting the *ALP* gene (583 bp)[12] of *A. fumigatus* was chosen for our study. In addition, *Afut-1* gene (245 bp)[18] was also chosen from retrotransposons of *A. fumigatus* for that estimated favorable specificity. For the probe-labeling assay, no agreeable outcome was gained from using nick translation technique, mostly due to fragmentation of DNA induced by the procedure (Fig. 2). Therefore, we employed either PCR fluorescein labeling mix (Rosche : 1636154) and Ulysis nucleic acid labeling kits (Molecular Probes : U-21652) which were carried out with an accordance to the manufacture's instructions. We also designed two more probes of PNA targeting the 26S rRNA of *C. albicans* and 28S rRNA of *Fusarium* species which were labeled at their N'-end with FITC (Greiner Bio-One Co. Ltd). PNA has been known as a novel type of DNA analogue[19] that has high sequence specificity and remarkable stability of both correct and mismatched PNA/DNA complexes[20-22]. In order to maximize sensitivity and specificity, we set the target of PNA probes on the rRNA derived from nuclear large subunit rDNA sequence. The sequences of nucleic acid used in the study are listed in Table 1. As a further advanced application, dual color fluorescent ISH (FISH) was carried out to visualize two different genes in a single section by adding two different probes targeting the *ALP* gene and the *Afut-1* gene to the hybridization buffer. At this time, *ALP* and *Afut-1* probes were labeled with Alexa 546 and FITC, respectively.

3. Pretreatment condition

To optimize ISH for sensitive and reproducible, a

ALP *Zygomycetes* *A. fumigatus*

Fig. 2. Labeling of DNA by nick translation with spectrum green linked nucleotide spoiling specificity of probe, mostly due to fragmentation.

Table 1. Nucleotide sequences of the primers and probes used in the study

Probe target	Nucleotide sequence	Probe length	Probe labeling
A. fumigatus Alkaline proteinase (*ALP*)	GCCTATCCGTGTACTTGATG AAGGTTCAGCACGATCAAC J Med Microbiol **49**: 285-290, 2000[12]	583 bp ds DNA	PCR: FITC or ULYSIS®: Alexa 546
A. fumigatus Retrotransposon (*Afut-1*)	CTTTGTCACATGCTCAGAAC GGTCCTAGCCAGCGATG Nucleic Acids Res **24**: 1428-1434, 1996[18]	245bp ds DNA	PCR: FITC
Fusarium spp. 28S rRNA	GATGATCAACCAAGCCCA Shinozaki M, Nakayama H, Shibuya K: unpublished data	18 mer PNA	N': FITC
C. albicans 26S rRNA	ACAGCAGAAGCCGTG J Clin Microbiol **39**: 4138-4141, 2001[21]	15 mer PNA	N': FITC

variety of pretreatment protocol was attempted with *Afut-1* probes and sections of formalin-fixed and paraffin-embedded tissue from mice infected with *A. fumigatus* as standard materials on the basis of result from our pilot study. We firstly examined whether pH of the heat solutions may influence the quality of ISH by using five different buffer solutions: 10 mM citrates (pH 6.0 and pH 7.0), 1 mM EDTA (pH 8.0), 0.65 mM Tris-HCl EDTA (pH 9.0), and 0.1 M Tris-HCl (pH 9.5). An efficacy of proteinase K digestion with each solution was also verified, simultaneously. In general, clinical specimens for histopathological examination are routinely fixed with formalin to provide better preservation of shape and structure of cells, matrix, and tissue of the specimen, but this has been cutting two ways, because the fixation causes cross-linking of proteins and fragmentation of DNA which generally reduces the penetration of nucleic acids probes. Therefore, an appropriate unmasking of target nucleic acids and ingenious probe design must be essential to take a successful result of ISH. The heating used in the study has been adapted from antigen retrieval technique used in conventional immunohistochemistry[23]. Although the heat solutions have empirically been used for ISH on formalin-fixed and paraffin-embedded sections[13, 14], the efficiency of the detection of fungus-specific nucleic acids in formalin-fixed and paraffin-embedded sections has not been systematically verified. Shi *et al.* previously documented that the pH of heat solution was an important factor for immunostaining to archival tissue sections[24]. As the result from our trial, following procedure produced a better outcome

Table 2. Verification of various pretreatment protocols

	−	Citrate (pH 6.0) or Proteinase K	Heat-treatment※ Citrate (pH 6.0)	Citrate (pH 7.0)	EDTA (pH 8.0)	TE (pH 9.5)	Tris-HCl (pH 9.0)
Ethanol-fixed cytological specimens (Cultured fungi)	+++	+++					
Papanicolaou stained cytological specimens (Cultured fungi)	++	+++					
Ethanol-fixed paraffin-embedded sections (Cultured fungi)	++	+++	+++				
Formalin-fixed paraffin-embedded sections (Tissue section)	−	+	+	+～++	++	++	++

※ The tissues following heat-treatment were subjected to proteinase K (10 μg/ml) treatments for 10 min.
Degree of fluorescent intensity is indicated as follows:
−: negative, +: weak, ++: definite, +++: intense.

for ISH that is to heat tissue sections in 10 mM EDTA (pH 8.0) at 98℃ for 30 min. followed by proteinase K digestion at 37℃ for 10 min. (Table 2).

4. Specificity verification of the probes

In order to verify the specificity of probes, sections of formalin-fixed and paraffin-embedded tissues were prepared from mice experimentally infected with six different fungi comprising *A. fumigatus*, *A. terreus*, *A. niger*, *S. apiospermum*, *M. circinelloides*, and *F. solani*. As the result, the *ALP* probe reacted strongly with *A. fumigatus* and weekly with both *A. niger* and *A. terreus* (Fig. 3a). On the contrary, *F. solani*, *C. albicans*, and *R. oryzae* showed no ISH signals (Fig. 3b). The *Afut-1* probe reacted specifically with *A. fumigatus*, and there were no ISH signals in tissues infected with *A. flavus*, *A. terreus*, *F. solani*, *C. albicans*, and *R. oryzae*. The result should be significantly useful to exclude *A. terreus* from other *Aspergillus* species because *A. terreus* is less susceptible to amphotericin B *in vitro* than others[25,26]. On the other hand, both the *C. albicans* and *Fusaium* species PNA probe specifically reacted with each fungus, respectively.

5. Practice of ISH

Two-color FISH method has been successfully accomplished (Fig. 4). An example of ISH is shown in Figure 5 utilizing *ALP* DNA and *C. albicans* PNA probe which was retrospectively carried out in a lesion from an autopsy case of which culture confirmed combined infection with *C. albicans* and *A. fumigatus* (Fig. 5). In addition, comparison with ISH and PCR is summarized in Table 3 using three autopsy cases *Aspergillus* infection, a case of *Zygomycetes* infection, and mice with *Fusarium* infection. We evaluated the supplemental utility of ISH conjunction with PCR for pathological diagnosis from formalin-fixed and paraffin-embedded tissue sections. Specific PCR was performed on formalin-fixed and paraffin-embedded tissue sections according to previously published techniques[8,27-29]. Fig. 6 shows the result of case #4 in Table 3. ISH showed more favorable sensitivity than PCR. Inadequately amplified PCR products surpassed at that of targeting DNA that caused false negative might explain the discrepancy. One possible reason may relate to our hypothesis that PCR-based method is affected easily by fragmentation of DNA due to formalin fixation and even if nucleic acids were suitably preserved, ISH can detect the target fungi by hybridizing to partially preserved nucleic acids. In addition, ISH may be overcome the disadvantage of PCR-based molecular techniques that has contamination risk and difficulty of DNA release in DNA extraction due to the rigid fungal cell wall.

In conclusion, ISH on formalin-fixed and paraffin-embedded tissue sections with invasive fungal infection is a valuable tool for the differentiation of medically important molds. In addition to details and careful observation on shape and distribution of mold in the

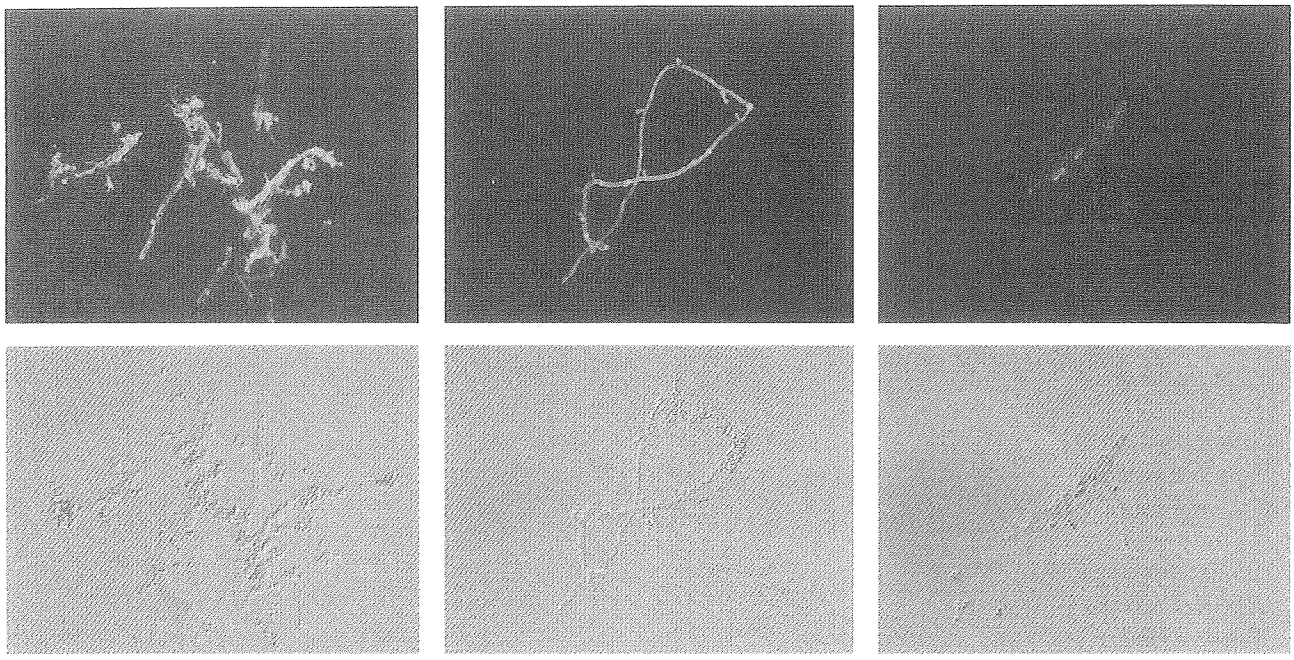

Aspergillus fumigatus *Aspergillus terreus* *Aspergillus niger*

(a)

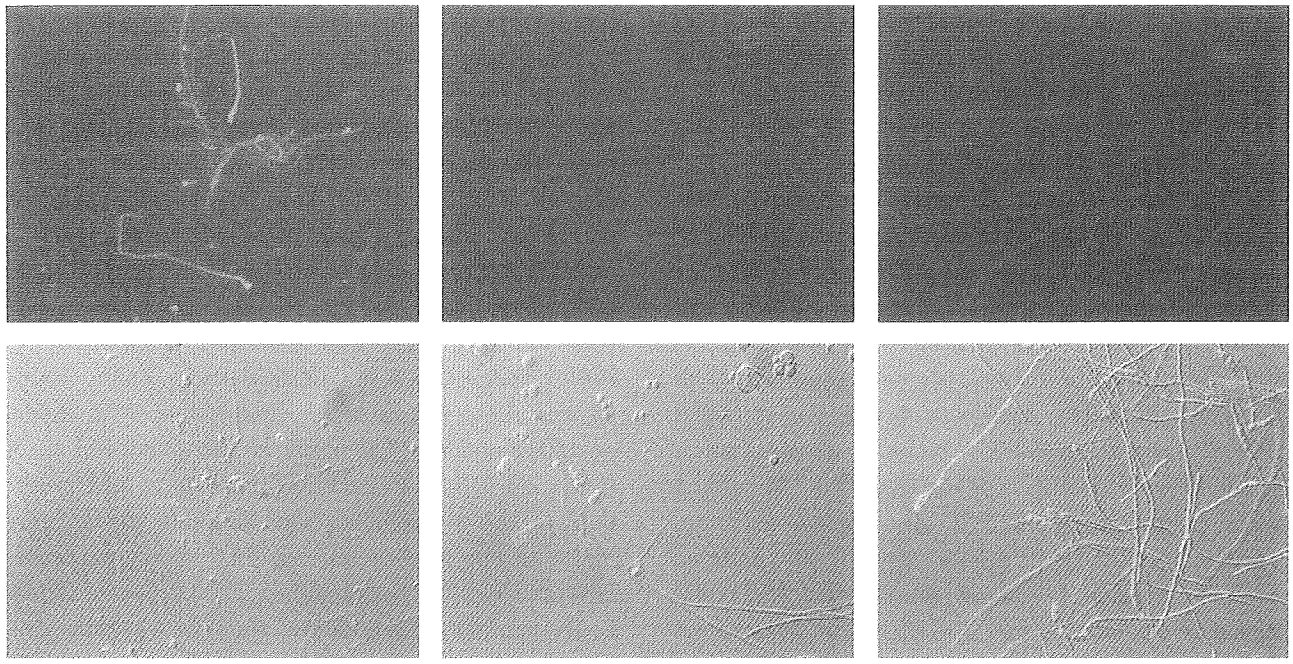

Scedosporium apiospermum *Mucor circinelloides* *Fusarium solani*

(b)

Fig. 3. Specificity verification of the probes.

Sections of formalin-fixed and paraffin-embedded tissues were employed in the study from mice infected with six different fungi comprising *A. fumigatus*, *A. terreus*, *A. niger*, *S. apiospermum*, *M. circinelloides*, and *F. solani*. As the result, the *ALP* probe reacted strongly with *A. fumigatus* and weekly with both *A. terreus*, *A. niger*, and *S. apiospermum* (a). On the contrary, *M.circinelloides* and *F. solani* showed no ISH signals (b).

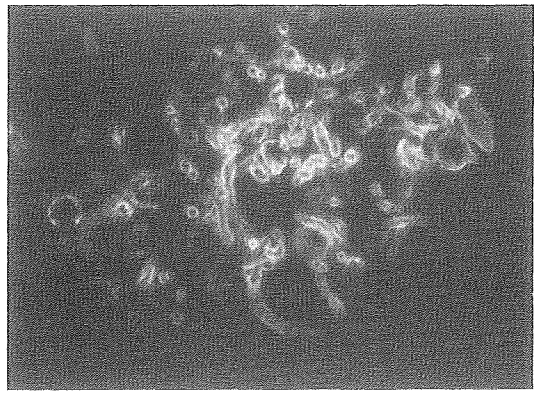

A . fumigatus

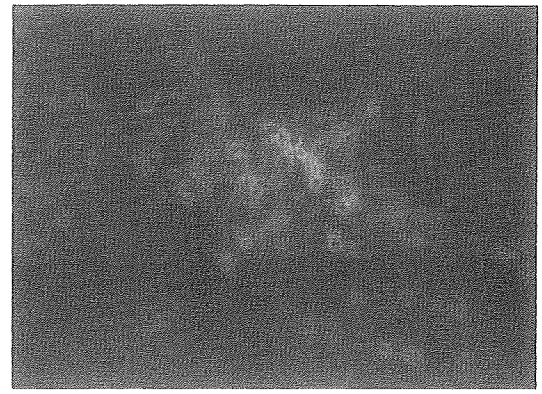

A . flavus

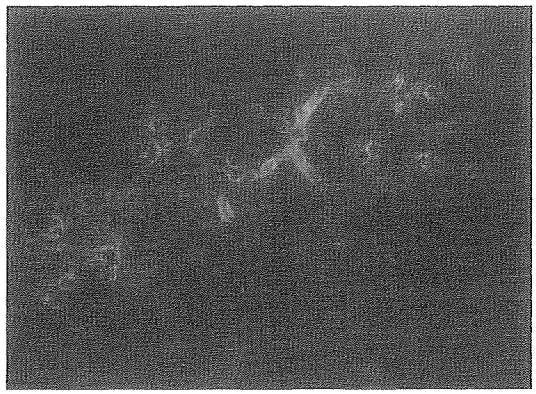

A. terreus

Fig. 4. Dual color fluorescent *in situ* hybridization.

Dual color (FISH) was carried out to visualize two different genes on a single section by adding two different probes targeting the *ALP* gene and the *Afut-1* gene to the hybridization buffer. At this photograph, *ALP* and *Afut-1* probes were labeled with Alexa 546 and FITC, respectively.

The PCR probe targeting the *ALP* gene of *A. fumigatus*

The PNA probe targeting the 26S rRNA *of C. albicans*

Fig. 5. An example of ISH utilizing *ALP* DNA and *C. albicans* PNA probe showing clear identification between *C. albicans* and *A. fumigatus* on the section of combined infection from an autopsy.

Table 3. Comparison between ISH and PCR

Case	Age/sex	Organs	Underlying disease	Diagnosis	*Afut-1*	*ALP*	ISH ALPns ALPnr	ISH LTR1n LTR2n	PCR AFU5S AFU5AS	PCR P58SL P28SL	PCR ZM1 ZM3	PCR Pbo1 SP2
1	57/M	Brain	AML (M2)	Zygomycosis	−	−	−	−	−	−	+	−
2	54/M	Lung	AML (M2)	IPA	+	+	−	−	−	−	−	−
3	37/F	Lung	CML	IPA	+	+	−	−	+	−	−	−
4	57/F	Lung	NHL	IPA	+	+	−	+	+	−	−	−
5	Experimental invasive fusariosis Lung				−	−	−	−	−	+	−	−
6	69/M	Lung	AML (M5)	IPA	/	+	/	/	+	/	−	/
				Zygomycosis	/	−	/	/	−	/	+	/

IPA: Invasive Pulmonary Aspergillosis, AML: Acute Myeloid Leukemia,
CML: Chronic Myelogenous Leukemia, NHL: Non Hodgkin's Lymphoma,

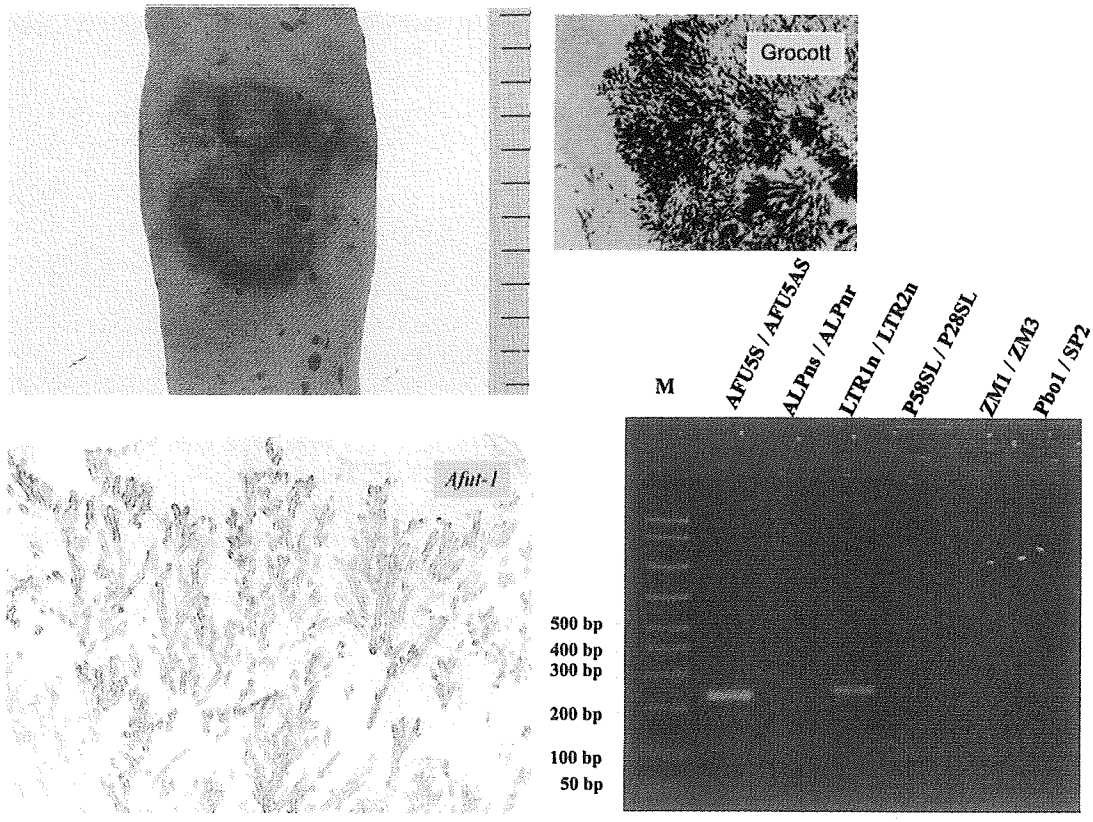

Fig. 6. Case #4 in Table 3. ISH shows more favorable sensitivity than PCR. Section of the lung, microphotograph of section stained with Grocott's, result of ISH with *Afut-1*, and PCR are shown from the left upper to the right lower corner.

tissue sections, ISH targeting specific DNA and rRNA of mold must provide an significant contribution to rapid and accurate diagnosis of the disease. An additional goal of our study should be to design probes against *Scedosporium* species and Zygomycetes.

ACKNOWLEDGEMENTS

This work was supported by the Health Science Research Grants for Research on Emerging and Re-emerging Infectious Diseases (H16-Shinko-6 and H19-Shinko-8) and Measures for Intractable Diseases (H20 nannchi ippann 35) from Ministry of Health, Labour and Welfare of Japan, and by Grant of the Strategic Basis on Research Grounds for Non-governmental Schools at Heisei 20th from Ministry of Education, Culture, Sports, Science and Technology-Japan to K. S.

We are grateful to Drs. K. Makimura, K. Uchida, J.P. Latgé and H. Yamaguchi for providing kind and important advices.

References

1) Anaissie EJ, Bodey GP, Rinaldi MG: Emerging fungal pathogens. Eur J Clin Microbiol Infect Dis **8**: 323-330, 1989.
2) McNeil MM, Nash SL, Hajjeh RA, Phelan MA, Conn LA, Plikaytis BD, Warnock DW: Trends in mortality due to invasive mycotic diseases in the United States, 1980-1997. Clin Infect Dis **33**: 641-647, 2001.
3) Shibuya K, Paris S, Ando T, Nakayama H, Hatori T, Latge JP: Catalases of *Aspergillus fumigatus* and inflammation in aspergillosis. Jpn J Med Mycol **47**: 249-255, 2006.
4) Lin SJ, Schranz J, Teutsh SM: Aspergillosis case-fatality rate: systematic review of the literature. Clin Infect Dis **32**: 358-366, 2001.
5) Shibuya K, Ando T, Hasegawa C, Wakayama M, Hamatani S, Hatori T, Nagayama T, Nonaka H: Pathophysiology of pulmonary aspergillosis. J Infect Chemother **10**: 138-145, 2004.
6) Makimura K, Murayama SY, Yamaguchi H: Detection of a wide range of medically important fungi by the polymerase chain reaction. J Med Microbiol **40**: 358-364, 1994.
7) Klingspor L, Jalal S: Molecular detection and identification of *Candida* and *Aspergillus* spp. from clinical samples using real-time PCR. Clin Microbiol Infect **12**: 745-753, 2006.
8) Skladny H, Buchheidt D, Baust C, Krieg-Schneider F, Seifarth W, Leib-Mösch C, Hehlmann R: Specific detection of *Aspergillus* species in blood and bronchoalveolar lavage samples of immunocompromised patients by two-step PCR. J Clin Microbiol **37**: 3865-3871, 1999.
9) Einsele H, Hebart H, Roller G, Löffler J, Rothenhofer I, Müller CA, Bowden RA, van Burik J, Engelhard D, Kanz L, Schumacher U: Detection and identification of fungal pathogens in blood by using molecular probes. J Clin Microbiol **35**: 1353-1360, 1997.
10) Lau A, Chen S, Sorrell T, Carter D, Malik R, Martin P, Halliday C: Development and clinical application of a panfungal PCR assay to detect and identify fungal DNA in tissue specimens. J Clin Microbiol **45**: 380-385, 2007.
11) Sandhu GS, Kline BC, Stockman L, Roberts G D: Molecular probes for diagnosis of fungal infections. J Clin Microbiol **33**: 2913-2919, 1995.
12) Hanazawa R, Murayama SY, Yamaguchi H: *In-situ* detection of *Aspergillus fumigatus*. J Med Microbiol **49**: 285-290, 2000.
13) Hayden RT, Qian X, Roberts GD, Lloyd RV: *In situ* hybridization for the identification of yeastlike organisms in tissue section. Diagn Mol Pathol **10**: 15-23, 2001.
14) Hayden RT, Qian X, Procop GW, Roberts GD, Lloyd RV: *In situ* hybridization for the identification of filamentous fungi in tissue section. Diagn Mol Pathol **11**: 119-126, 2002.
15) Montone KT, Litzky LA: Rapid method for detection of *Aspergillus* 5S ribosomal RNA using a genus-specific oligonucleotide probe. Am J Clin Pathol **103**: 48-51, 1995.
16) Kobayashi M, Sonobe H, Ikezoe T, Hakoda E, Ohtsuki Y, Taguchi H: *In situ* detection of *Aspergillus* 18S ribosomal RNA in invasive pulmonary aspergillosis. Intern Med **38**: 563-569, 1999.
17) Zimmerman RL, Montone KT, Fogt F, Norris AH: Ultra fast identification of *Aspergillus* species in pulmonary cytology specimens by *in situ* hybridization. Int J Mol Med **5**: 427-429, 2000.
18) Neuveglise C, Sarfati J, Latge JP, Paris S: *Afut1*, a retrotransposon-like element from *Aspergillus fumigatus*. Nucleic Acids Res **24**: 1428-1434, 1996.
19) Nielsen PE, Egholm M, Berg RH, Buchardt O: Sequence-selective recognition of DNA by strand displacement with a thymine-substituted polyamide. Science **254**: 1497-1500, 1991.
20) Wilson DA, Joyce MJ, Hall LS, Reller LB, Roberts GD, Hall GS, Alexander BD, Procop GW: Multicenter evaluation of a *Candida albicans* peptide nucleic acid fluorescent *in situ* hybridization probe for characterization of yeast isolates from blood cultures. J Clin Microbiol **43**: 2909-2912, 2005.
21) Oliveira K, Haase G, Kurtzman C, Hyldig-Nielsen JJ, Stender H: Differentiation of *Candida albicans* and *Candida dubliniensis* by fluorescent *in situ* hybridization with peptide nucleic acid probes. J Clin Microbiol **39**: 4138-4141, 2001.
22) Demidov VV, Yavnilovich MV, Belotserkovskii BP, Frank-Kamenetskii MD, Nielsen PE: Kinetics and mechanism of polyamide ("peptide") nucleic acid binding to duplex DNA. Proc Natl Acad Sci USA **92**: 2637-2641, 1995.
23) Shi SR, Key ME, Kalra KL: Antigen retrieval in formalin-fixed, paraffin-embedded tissues: an enhancement method for immunohistochemical staining based on microwave oven heating of tissue sections. J Histochem Cytochem **39**: 741-748, 1991.
24) Shi SR, Imam SA, Young L, Cote RJ, Taylor CR: Antigen retrieval immunohistochemistry under the influence of pH using monoclonal antibodies. J Histochem

Cytochem **43**: 193-201, 1995.
25) Lass-Flörl C, Kofler G, Kropshofer G, Hermans J, Kreczy A, Dierich MP, Niederwieser D: *In-vitro* testing of susceptibility to amphotericin B is a reliable predictor of clinical outcome in invasive aspergillosis. J Antimicrob Chemother **42**: 497-502, 1998.
26) Sutton DA, Sanche SE, Revankar SG, Fothergill AW, Rinaldi MG: *In vitro* amphotericin B resistance in clinical isolates of *Aspergillus terreus*, with a head-to-head comparison to voriconazole. J Clin Microbiol **37**: 2343-2345, 1999.
27) Hue FX, Huerre M, Rouffault MA, de Bievre C: Specific detection of *Fusarium* species in blood and tissues by a PCR technique. J Clin Microbiol **37**: 2434-2438, 1999.
28) Bialek R, Konrad F, Kern J, Aepinus C, Cecenas L, Gonzalez GM, Just-Nübling G, Willinger B, Presterl E, Lass-Flörl C, Rickerts V: PCR based identification and discrimination of agents of mucormycosis and aspergillosis in paraffin wax embedded tissue. J Clin Pathol **58**: 1180-1184, 2005.
29) Hagari Y, Ishioka S, Ohyama F, Mihara M: Cutaneous infection showing sporotrichoid spread caused by *Pseudallescheria boydii* (*Scedosporium apiospermum*): successful detection of fungal DNA in formalin-fixed, paraffin-embedded sections by seminested PCR. Arch Dermatol **138**: 271-272, 2002.

Jpn. J. Infect. Dis., 61, 450-453, 2008

Original Article

Pathophysiological Study of Chronic Necrotizing Pulmonary Aspergillosis

Keishi Sugino, Chikako Hasegawa[1], Go Sano, Kazutoshi Shibuya[1]* and Sakae Homma

Department of Respiratory Medicine and [1]Department of Pathology, Toho University Omori Medical Center, Tokyo 143-8541, Japan

(Received April 1, 2008. Accepted August 15, 2008)

SUMMARY: The aim of the present study is to define the characteristics of the clinical and histopathological features of chronic necrotizing pulmonary aspergillosis (CNPA) cases with severe hemoptysis. We conducted a histological study of three patients clinically diagnosed as having CNPA who had hemoptysis for 5 years. A tuberculosis sequelae was found as the underlying disorder in all three cases. All patients had fever, general fatigue, and hemoptysis, and their chest computed tomographic images revealed fungus balls, cavity wall thickening, consolidation surrounding the cavity, and satellite foci. All had been treated with anti-fungal drugs and corticosteroids. However, all patients died from respiratory failure due to massive hemoptysis. Histopathological examination revealed that the cavity wall consisted of three layers comprised of necrotic, granulation, and fibrous tissue layers. *Aspergilli* were found in both the fungus ball and necrotic tissue comprising the inner layer of the cavity. In addition, most of the vessels were incompletely occluded with thrombosis and were necrotic, as well as showing local invasion of *Aspergilli*. Surgical intervention should be considered as a prior procedure for CNPA patients, because vessels at the cavity wall, whether occluded completely or incompletely, are usually necrotic and/or show local invasion of *Aspergilli*.

INTRODUCTION

Binder et al. (1) defined the term chronic necrotizing pulmonary aspergillosis (CNPA) to describe the state between aspergilloma and invasive pulmonary aspergillus. Although several recent reports have led to a better understanding of the clinical features of CNPA (2), its pathological features and mechanisms of hemoptysis still remain obscure. To obtain a detailed understanding of the pathophysiology of CNPA and hemoptysis as its serious complication, both the clinical courses and histological alterations observed in three autopsies of CNPA were examined. These three cases had been transferred from non-invasive aspergillosis of fungal ball type occurred in sequelae of pulmonary tuberculosis.

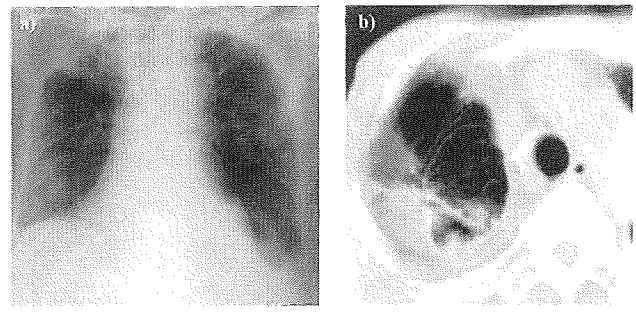

Fig. 1. (a) Chest radiograph on admission showed pleural thickening in the right upper lung field (Case 1). (b) Chest CT showed a mycetoma of 20×18 mm in size within the cavity, the wall of which was thickened and had invaded the surrounding parenchyma (Case 1).

PATIENTS AND LABORATORY INFORMATION

Case 1: A 67-year-old man with sequelae of pulmonary tuberculosis and hepatitis C virus (HCV)-related liver cirrhosis was admitted to our hospital in October 2001 with a 4-month history of cough, hemoptysis, wheezing, and dyspnea. Physical examination revealed a body temperature of 37.4°C, blood pressure of 134/86 mmHg, and pulse rate of 68/min with an irregular rhythm. The auscultation indicated wheezing in the bilateral lung fields. The laboratory data revealed a leukocyte count of 3,800/μl with 62.5% neutrophils, a platelet count of 9.4 × $10^3/\mu$l, and PaO_2 of 64 torr and $PaCO_2$ of 62 torr on room air. Serum precipitation antibody for *Aspergillus* was positive, and β-D-glucan was elevated at 247 pg/ml. *Aspergillus* galactomannan was not examined. The chest X-ray showed pleural thickening in the right upper lung field (Fig. 1a). Chest computed tomography (CT) scan revealed a mycetoma of 20 × 18 mm in size within the thick-walled cavity which was encompassed with consolidation (Fig. 1b). No mycetomas were isolated from the sputum and no fungal, bacterial, and mycobacterial pathogens were found. He was started with a single 200-mg dose of oral itraconazole (ITCZ) and 40-mg dose of prednisolone for complications of bronchial asthma. On the 20th day after the initiation of the treatment, chest X-ray revealed progressive ground glass opacities in the bilateral lower lung fields. He was administered a high dose of intravenous corticosteroid under the diagnosis of suspected drug-induced ITCZ-induced interstitial pneumonia. After receiving intravenous corticosteroid pulse therapy, the clinical symptoms and chest CT images temporarily improved. However, on the 80th day, the patient died of respiratory failure caused by massive hemoptysis.

Case 2: A 77-year-old man with sequelae of pulmonary tuberculosis was admitted to our hospital in March 2000 with a 4-month history of fever, hemoptysis, and dyspnea. He had been treated with oral antibiotics beginning 3 months before admission. The chest X-ray showed a cavity in the left upper lung field. Physical examination revealed a body temperature of 38.2°C, blood pressure of 110/64 mmHg, and pulse rate of 96/min with regular rhythm. The auscultation indi-

*Corresponding author: Mailing address: Department of Pathology, Toho University Omori Medical Center, Omori-nishi 6-11-1, Ota-ku, Tokyo 143-8541, Japan. Tel: +81-3-3762-4151, Fax: +81-3-3766-3551, E-mail: kaz@med.toho-u.ac.jp

cated coarse crackles in the bilateral lung fields. Laboratory data revealed a leukocyte count of 7,200/μl with 82.5% neutrophils, PaO_2 of 64 torr and $PaCO_2$ of 62 torr on 50% oxygen mask. Sputum culture isolated *Mycobacterium avium* complex. The serum precipitation antibody for *Aspergillus* was positive, and β-D-glucan and galactomannan were elevated at 21.8 pg/ml and 2.5 ng/ml, respectively. Chest X-ray showed a cavity with thickening of the adjacent pleura in the left upper lung field and consolidation in the right upper and middle lung fields (Fig. 2a). Chest CT scan revealed a mycetoma of 28 × 18 mm in size within the cavity, and the consolidation was confirmed with air bronchograms (Figs. 2b, 2c). He was started with a single 10-mg dose of intravenous AMPH-B (amphotericin-B deoxycholate 0.25 mg/kg body weight), 200-mg of oral ITCZ, 200-mg of oral sparfloxacin, and 800-mg of oral erythromycin. After the initiation of these treatments, the clinical symptoms improved and the chest CT showed significant improvement of consolidation and a decrease in the size of the mycetoma. Just before death, no acid-fast bacilli were found in the sputum. However, on the 44th day after treatment, he died of refractory respiratory failure caused by the sudden onset of massive hemoptysis.

Case 3: A 77-year-old woman with sequelae of pulmonary tuberculosis and HCV-related liver cirrhosis was admitted to our hospital in March 2004 with a 1-month history of fever, hemoptysis, and dyspnea. She had a temperature of 37°C, blood pressure of 134/70 mmHg, and pulse rate of 90/min with a regular rhythm. The chest auscultation revealed coarse crackles in the bilateral lung fields. Laboratory data revealed a leukocyte count of 11,500/μl with 70.5% neutrophils, a platelet count of 9.4 × $10^3/\mu$l, and PaO_2 of 54 torr and $PaCO_2$ of 42 torr on room air. Culture of sputum was negative for fungal, bacterial, or mycobacterial pathogens. Serum precipitation antibody for *Aspergillus* was positive and β-D-glucan was elevated at 27.4 pg/ml, but galactomannan was not elevated (0.2 ng/ml). Chest X-ray showed a cavity with adjacent pleural thickening in the right upper lung field and consolidation in the right upper and middle lung fields (Fig. 3a). Chest CT scan revealed a cavity of 70 × 55 mm in size and the consolidation was confirmed (Figs. 3b, 3c). She had been treated with a single 150-mg dose of micafungin and 20-mg of prednisolone for the organizing pneumonia. After the initiation of antifungal treatment, the clinical symptoms and chest CT findings were improved. However, on the 37th day the patient died of respiratory failure resulting from massive hemoptysis.

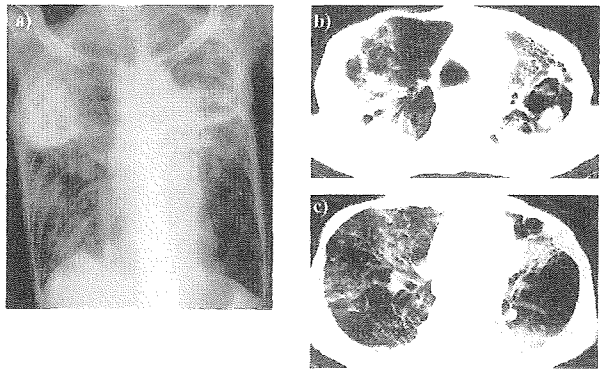

Fig. 2. (a) Chest radiograph revealed a cavitary lesion in the left upper lung field and infiltrative shadow in the right upper and middle lung fields (Case 2). (b), (c) Chest CT showed a fungus ball in the cavity in the left upper lobe and consolidation in the right upper and middle lobes (Case 2).

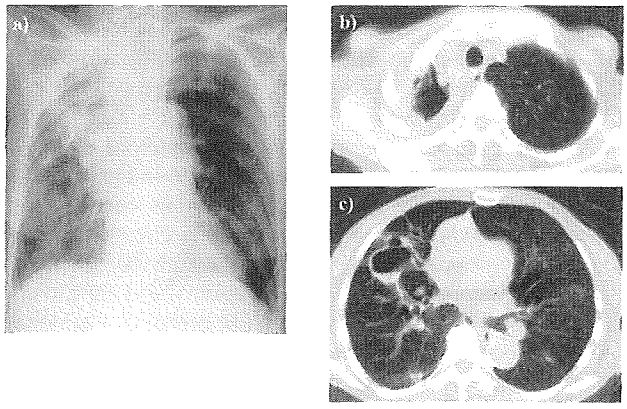

Fig. 3. (a) Chest radiograph showing a cavitary lesion in the right upper lung field and infiltrative shadow surrounding the cavitation (Case 3). (b), (c) Chest CT scan showing a cavity with adjacent pleural thickening in the right upper lobe and cavitary infiltrates with fluid collection in the middle lobe (Case 3).

RESULTS

Case 1: Macroscopic examination of the right upper lobe revealed a cavity of 50 mm in diameter, which was filled with a fungus ball and coagulated exudate (Fig. 4a). Histological examination revealed that the cavity wall was composed of three concentric circular layers: necrotic, granulation, and fibrous tissue layers arranged from the luminal position (Fig. 4b). Numerous hyphae were present in the fungus ball and necrotic tissue, and some had invaded into blood vessels (Fig. 4c).

Case 2: Macroscopically, a cavity measuring 50×40 mm in size was found at the section of the left upper lobe which was filled with coagulated bloody exudate corresponding to a mycetoma (Fig. 5a). Numerous hyphae were confirmed by histological examination in the coagulation of exudate (Fig. 5b). However, a few hyphae were seen as invading organisms into the blood vessels wall (Fig. 5c).

Case 3: Macroscopic examination showed a thin-walled

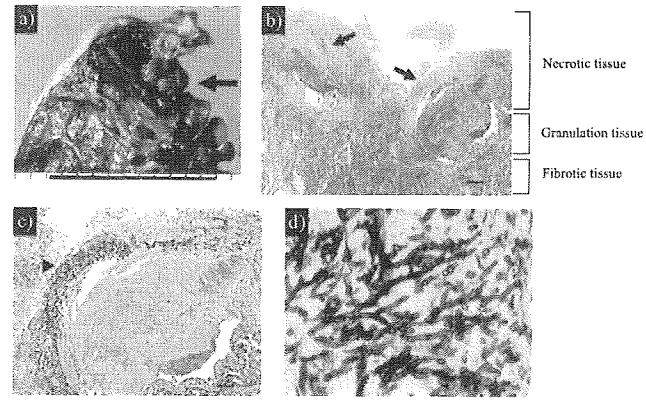

Fig. 4. (a) Macroscopic appearance of the right upper lobe demonstrated a cavity 50 mm in diameter, which was filled with a fungus ball and necrotic materials (arrow) (Case 1). Scale: 1 division = 0.5 cm. (b) Histopathological appearance of the cavity wall revealed three layers, which were of necrotic, granulation and fibrotic tissue (arrows) (Hematoxylin-Eosin stain). Scale bar = 250 μm. (c) Many fungi had invaded the blood vessel (arrow head) (Grocott's stain). Scale bar = 200 μm. (d) There were numerous *Aspergillus* hyphae with Y-shaped branching.

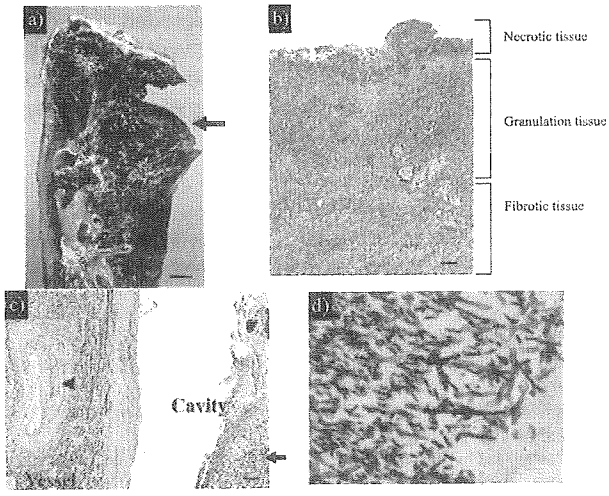

Fig. 5. (a) Macroscopic examination of the left upper lobe revealed a cavity 5 cm in diameter, which was filled with a fungus ball and necrotic materials (arrow) (Case 2). Scale bar = 1 cm. (b) Histopathology of the cavity wall revealed three layers: necrotic, granulation, and fibrotic tissue (Hematoxylin-Eosin stain). Scale bar = 150 μm. (c) Many fungi were evident in the fungus ball and in the cavity (arrow), and had invaded into blood vessel (arrow head) (Grocott's stain). Scale bar = 200 μm. (d) There were densely intertwined separated hyphae consistent with *Aspergillus* spp.

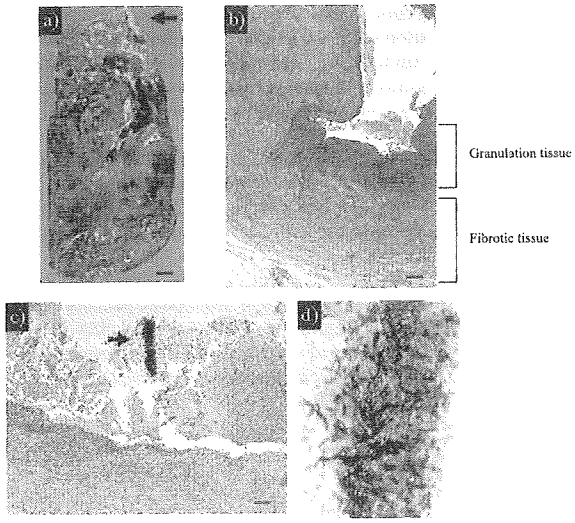

Fig. 6. (a) Macroscopic examination of the right upper lobe revealed a cavity wall 70 mm in diameter (arrow) (Case 3). Scale bar = 1 cm. (b) Microscopic examination of the cavity wall revealed two layers, which were granulation tissue and fibrotic tissue, and the absence of necrotic tissue (Hematoxylin-Eosin stain). Scale bar = 300 μm. (c) Some fungi were noted in the fungus ball (arrow) (Grocott's stain). Scale bar = 170 μm. (d) Fungal elements, showing the branching separated *Aspergillus* hyphae.

cavity of 70 mm in diameter on the section of the right upper lobe (Fig. 6a). Histologically, the cavity wall was comprised of thin and dense fibrous tissue covered with a little necrotic material (Fig. 6b). No hyphae were found as invading organisms in the cavity wall. Hyphae of fungi were limited in the intracavitary mycetoma in the case (Fig. 6c). No fungi were also found in the organizing lesions corresponding to the area of consolidation around the cavity on the chest X-ray.

DISCUSSION

Binder et al. (1) proposed that CNPA is a disease pattern that is independent of the pulmonary aspergillosis that characteristically develops in patients with mild immunosuppression, including those with diabetes mellitus, malnutrition, long-term use of low-dose corticosteroids, and collagen vascular diseases such as ankylosing spondylitis and rheumatoid arthritis. Although the clinical course is a chronic process that progresses slowly over several months to years, cavitations occur continuously due to hyphae invading into the tissues, and there is no vascular invasion or dissemination to other organs. This was followed by Gefter et al. (3), who defined semi-invasive aspergillosis as a lesion accompanied by destruction of the lung without fungus invasion of the tissues. As previously mentioned, this form may be accepted as the state during which transformation from the non-invasive form to invasive pulmonary disease occurs.

CNPA usually occurs in middle-aged and elderly patients with underlying lung diseases inducing anatomical remodeling of peripheral airways, such as in chronic obstructive pulmonary disease (COPD), old tuberculosis, pneumoconiosis, cystic fibrosis, and sarcoidosis, and is more likely to develop if the previous anatomical alteration has progressed, such as with inactive tuberculosis with residual cavities (4). The patient usually has fever, cough, sputum, and weight loss of 1 to 6 months duration (4). Radiographic findings show progressive upper lobe cavitary infiltrates associated with pleural thickening. Mycetomas are seen in about half of the patients (5). In the present study, the mean age of the three patients examined was 73.7 ± 8.8 years old. The underlying pulmonary disorders were sequelae of pulmonary tuberculosis in all patients, and two had HCV-related liver cirrhosis as the systemic underlying disease. All presented with chronic cough, hemoptysis, fever, and dyspnea. Chest radiograph revealed a cavity filled with a fungus ball at the upper lobes as a common finding in all patients. Although various histopathological alterations of CNPA have been reported, no histopathological definition has been accepted for diagnosis (2). Therefore, in the present study, the three patients with CNPA were clinically diagnosed in accordance with criteria proposed by Kohno et al. (6). The criteria are: (i) chronic symptoms with fever, cough, hemoptysis, and body weight loss, (ii) chest X-ray and CT scan abnormalities showing infiltrates and cavities in the upper lobes, (iii) positive levels of serum precipitation antibody for *Aspergillus* and β-D-glucan; and/or, (iv) isolation of *Aspergillus* spp. from lung specimens, and (v) failure to detect other bacterial, fungal, or mycobacterial pathogens. According to these criteria, the three patients were diagnosed as having CNPA.

Our pathological examination confirmed fungus balls, including necrotic material within the cavity in which numerous fungi were present. There was, however, an absence of dissemination to other organs observed by autopsy examination. In addition, the lungs in all present cases showed no histopathological findings of bronchopneumonia or nontuberculosis mycobacterial pulmonary disease.

Consequently, this suggested that the organization around the cavity may be caused by degenerated exudate disseminated and provided from the mycetoma in the cavity via the airway. The presence of an organizing lesion without fungal components around the cavity is a significantly different characteristic from that of invasive pulmonary aspergillosis (IPA), because the infiltrative shadow in the case of IPA essentially mirrors the filling of acute inflammatory exudates in the alveoli with a fungal proliferation (7,8). Protease and other considerable cytotoxic agents produced by *Aspergilli* (9,10)

may also play a role in producing and increasing the organizing lesion in CNPA. It has been known that long-term corticosteroid administration, diabetes mellitus, and liver cirrhosis impair the function of neutrophils, which play an important role in preventing the invasion of the hyphae of *Aspergilli* from the cavity to the wall covered with epithelium (11).

All of the present patients died of respiratory failure caused by massive hemoptysis. It has been known that massive hemoptysis in the case of IPA is caused by destruction of vessels by direct invasion of *Aspergilli*. However, hemoptysis, understood as bleeding of the peripheral airway, in CNPA may result from invasion of *Aspergilli* in the vessels walls which is limited in necrotic layer of the cavity wall and that lumen is largely occluded by thrombi. Hebisawa et al. (12) reported that hemoptysis occurred in patients with CNPA caused by rupturing of the pulmonary artery, which had been exposed to the luminal surface of the cavity. They assumed that fibrinoid necrosis may weaken the pulmonary arterial wall and that high blood pressure from the bronchial and intercostal arteries may cause the pulmonary artery to rupture. From our observation, an exposure of blood vessels was confirmed, but most of them were occluded incompletely by thrombosis. Therefore, destruction of a plural number of vessels involved by necrosis, local invasion of *Aspergilli*, and the break down of necrotic tissue itself into the cavity may cause bleeding. Moreover, coagulation abnormalities due to liver cirrhosis revealed by the patients of Cases 1 and 3 might be the trigger for hemoptysis.

We surmised that although the clinical signs and data indicate that fungal growth is restrained by antifungal therapy, the patient still is at continuous risk for sudden onset of massive hemoptysis, because the blood vessels, even if they are mostly occluded, may be exposed to the lumen and progressively degenerated by involvement of necrosis at the cavity wall. A coagulation abnormality is commonly associated with such patients. Thus, pulmonary resection is one of the agreeable procedure to improve the outcome for patients with IPA with neutropenia (13,14).

In conclusion, surgical intervention should be considered as a prior procedure for the disease, even though the invasion of *Aspergilli* is essentially limited to the eroded and necrotic area of the cavity wall in CNPA, because vessels at the cavity wall, whether occluded completely or incompletely, are usually involved by necrosis and/or local invasion of *Aspergilli*, as confirmed by the present study.

REFERENCES

1. Binder, R.E., Faling, L.J., Pugatch, R.D., et al. (1982): Chronic necrotizing pulmonary aspergillosis: a discrete clinical entity. Medicine, 61, 109-124.
2. Yousem, S.A. (1997): The histological spectrum of chronic necotizing forms of pulmonary aspergillosis. Hum. Pathol., 28, 650-656.
3. Gefter, W.B., Weingrad, T.R., Epstein, D.M., et al. (1981): Semi-invasive pulmonary aspergillus. Radiology, 140, 313-321.
4. Soubani, A.O. and Chandrasekar, P.H. (2002): The clinical spectrum of pulmonary aspergillosis. Chest, 121, 1988-1999.
5. Saraceno, J.L., Phelps, D.T., Ferro, T.J., et al. (1997): Chronic necrotizing pulmonary aspergillosis: approach to management. Chest, 112, 541-548.
6. Kohno, S., Masaoka, T., Yamaguchi, H., et al. (2004): A multicenter, open-label clinical study of micafungin (FK463) in the treatment of deep-seated mycosis in Japan. Scand. J. Infect. Dis., 36, 372-379.
7. Shibuya, K., Ando, T., Wakayama, M., et al. (1997): Pathological spectrum of invasive pulmonary aspergillosis. Jpn. J. Med. Mycol., 38, 175-181 (in Japanese).
8. Sugino, K., Hasegawa, T., Kimura, K., et al. (2007): Clinicopathological study of invasive pulmonary aspergillosis complicated by leukemia. J. Jpn. Assoc. Infect. Dis., 81, 261-267 (in Japanese).
9. Amitani, R., Taylor, G., Elezis, E.N., et al. (1995): Purification and characterization of factors produced by aspergillus fumigatus which affect human clinical respiratory epithelium. Infect. Immun., 63, 3266-3271.
10. Murayama, T., Amitani, R., Ikegami, Y., et al. (1996): Suppressive effects of aspergillus fumigatus culture filtrates on human alveolar macrophages and polymorphonuclear leucocytes. Eur. Respir. J., 9, 293-300.
11. Shibuya, K., Ando, T., Hasegawa, C., et al. (2004): Pathophysiology of pulmonary aspergillosis. J. Infect. Chemother., 10, 138-145.
12. Hebisawa, A., Tamura, A., Baba, M., et al. (2003): Histopathology of saprophytic aspergillosis, including hemoptysis. Jpn. J. Chest Dis., 62, 1070-1079 (in Japanese).
13. Reichenberger, F., Habicht, J., Kaim, A., et al. (1998): Lung resection for invasive pulmonary aspergillosis in neutropenic patients with hematologic diseases. Am. J. Respir. Crit. Care Med., 158, 885-890.
14. Pidhorecky, I., Urschel, J. and Anderson, T. (2000): Resection of invasive pulmonary aspergillosis in immunocompromised patients. Ann. Surg. Oncol., 7, 312-317.

Jpn. J. Med. Mycol.
Vol. 51, 000 - 000, 2010
ISSN 0916 - 4804

Original Articles

Histopathological Study of Candidal Infection in the Central Nervous System

Haruo Nakayama[1], Kazutoshi Shibuya[2*], Masatomo Kimura[3], Satoshi Iwabuchi[1], Morikazu Ueda[1]

[1]2nd Department of Neurosurgery and [2]Department of Surgical Pathology, [3]Department of Pathology, Kinki University School of Medicine, Toho University school of Medicine, Tokyo 143-8541, Japan

〔Received : 8, December 2009. Accepted : 7, December 2009.〕

In recent years, incidence of invasive fungal infection has been increasing, mostly due to advance of medicine that may produce immunocompromised individuals. Candidial infection in central nervous system (CNS) is one of the most serious forms of blood stream infection of *Candida* sp. of which mortality has been known as more than 50%.

In this research, we employed 27 autopsies with invasive CNS yeast infection which were confirmed. In addition to detailed morphological analysis of yeast cells in lesions, *in situ* hybridization was carried with originally designed *Candida*-specific peptide nucleic acid (PNA) probe to identify candidial infection of each patient. This was followed by histopathological investigation; invasiveness, shape, and distribution of yeast or yeasts with pseudohyphal growth, and a study regarding to correlation between histological characteristics and number of leukocyte in the peripheral blood just before death.

As a result, supratentorial region was the commonest area of disseminated candidial infection in CNS, and that density was highest in the cerebral gray matter followed by the white matter and basal ganglia. On the other hand, regarding to the lesions developed in the cortical area, the average distance from the brain surface was 4.026 mm. This area corresponding to deeper cortex has a characteristic arterial structure that refers hair-pig curving reverse. The structure may attribute to high incidence of development of candidial foci in the deeper cortex, because of that increasing of shear stress.

Key words : Candidal Infection in the Central Nervous System, in situ hybridization, Invasive fungal infection

Introduction

Many powerful, contemporary medical therapies-including chemotherapy, solid organ and hematopoietic stem cell transplantation, and the implantation of medical devices are associated with an immunocompromised state[1,2]. As a result, opportunistic infections caused by low-virulence or commensal microorganisms are among the most important complications of such therapies and may significantly influence the prognoses of underlying diseases. In particular, opportunistic invasive fungal infections are extensively serious because of the difficulties in diagnosis and limited number of effective treatment options[3,4].

Address for correspondence : Kazutoshi Shibuya
Department of Surgical Pathology, Toho University School of Medicine,
6-11-1, Omori-Nishi, Ota-ku, Tokyo 143-8541 Japan

Candida spp. have been known as medically important pathogenic yeasts and the most common causes of blood stream infections, especially in surgery and critical-care medicine[5,6]. In addition, *Candida* spp. are the fourth commonest source of septicemia. Approximately half of patients with candidemia have fungal involvement of the central nervous system (CNS)[7] of which mortality ranges from 80% to 97%[8,9]. In addition, fungi cause 92% of brain abscess in recipients of hematopoietic stem cell transplants. In these cases, *Candida* spp. are the second commonest cause following *Aspergillus* spp.[10]. In spite of these high incidences, few reports have been published concerning the pathophysiology of CNS candidiasis. Such research can provide basic knowledge that is instrumental in establishing rapid and accurate diagnostic procedures.

In the present study, we performed detailed pathological examinations on CNS lesions from autopsies of patients with candidemia. The pathological examination

involved molecular identification of *Candida albicans* in paraffin-embedded tissue sections by *in situ* hybridization (ISH) to elucidate the pathophysiology, which mirrors clinical signs and radiological images.

Materials and Methods

Cases and ethical procedure

We searched the autopsy records of the Toho University Medical Center Omori Hospital from 1979 to 2007 for cases of either systemic fungal infections or brain abscesses. We histologically identified and included in the study 27 cases of systemic candidiasis, 10 cases of bacterial infection, 5 cases of aspergillosis and zygomycosis. One case of invasive trichosporonosis confirmed by culture was also employed as the negative control for *Candida albicans*-specific probe. The protocol used to examine these autopsies was reviewed and authorized by the ethics committee of Toho University School of Medicine (#19003).

Methods

1. Investigation of major clinical findings and clinical management

We searched the medical records of objective autopsies for the following information: underlying diseases, sex, age, use of antibiotics and adrenocorticosteroids, intravenous catheterization, results of blood culture, and white blood-cell counts in peripheral blood just before the death.

2. Histopathological examination

Sections (3 μm thick) were prepared from formalin-fixed and paraffin-embedded tissue from the autopsy, and were stained with both hematoxylin-eosin (HE) and periodic acid Schiff's (PAS) for histological examination. ISH was also applied to these sections. In cases of morphometric analysis described below in sections 2-2-2 and 2-2-3, HE-stained sections were digitally scanned (GT-X900, EPSON, Japan) and converted to digital files in the JPEG format. The length and area of the lesions were measured using a personal computer (PowerBook G4, Apple Co Ltd., Cupertino, CA, USA) with image analyzing software (Image J, downloaded from http://rsb.info.nih.gov/ij/).

2-1. Confirmation of *C. albicans* in paraffin-embedded tissue sections by ISH

2-1-1. Preparation of peptide nucleic acid (PNA) probes

C. albicans-specific PNA probe was prepared for the present study. It was prepared following the procedure described by Rigby S. *et al*[11]. Thus, the sequence processing was precisely performed with the computer processing software (Vector NTI Advance version 10.3.1, Invitrogen Corp, San Diego, CA, USA), and the 26S rRNA databases at the National Center for Biotechnology Information (http://www.ncbi.nlm.nih.gov/BLAST/) were searched for a specific sequence testing the probe specificity. The sequences were from 11 species within the *Candida* clade (Sugita and Nakase, 1999) as well as 10 other clinically relevant yeast species, mainly of the *Candida* genus. From these alignments, a specific probe sequence (AGAGAGCAGCATGCA) complementary to the 26S rRNA of *C. albicans* was identified. The probe (FASMAC Co., Ltd., Kanagawa, Japan) was designed to minimize any secondary structures. In addition, the target sequence was checked for specificity by comparison with sequences in the GenBank database by using an Advanced BLAST search (www.ncbi.nlm.nih.gov/blast)[12]. These two probes were labeled at their N'-end with fluorescein isothiocyanate (FITC; Roche Applied Sciences, Indianapolis, IN, USA).

2-1-2. ISH

Pretreatment of sections: 3-μm-thick paraffin sections were used for ISH hybridization. After deparaffinization and rehydration, sections were microwaved for 40 minutes in 10 mmol/L EDTA buffer solution (pH 8.0) and cooled to room temperature for 20 minutes. Then, the sections were rinsed three times in 10 × phosphate-buffered saline (PBS) for 5 minutes. Sections were then digested with 10 μg/mL proteinase K (Roche Diagnostics) in 10 mmol/L phosphate buffered saline (PBS; pH 7.2) for 10 minutes at 37 ℃, followed by post-fixation for 10 minutes with freshly prepared 4% paraformaldehyde phosphate buffer solution with 0.1 mol/L phosphate buffer (pH 7.4). Sections were rinsed three times in sterile purified water, digested in 0.2 N HCl for 10 minutes, rinsed three times in PBS at room temperature, and rinsed twice in sterile purified water. Sections then were dehydrated in graded ethanol solutions, followed by air-drying.

Hybridization and post hybridization washes: A species-specific PNA probe solution (1 ng/L in prehybridization buffer) was applied to sections. Slides were coverslipped with a Sigmacote® (Sigma, St. Louis, USA)-coated coverglass, heat-treated at 94℃ for 10 minutes, and hybridized in a humid environment for 90 minutes at 55℃. Sections were rinsed once in 2 × standard saline citrate (SSC) for 10 minutes at 50℃, washed twice in 0.5 × SSC for 20 minutes at 50℃ to remove excess probe, and rinsed three times in PBS for 5 minutes at room temperature.

Immunochemical detection: After repeated washings, the signals were detected by enzyme immunohistoche-

mistry using anti-FITC antibody (Roche Applied Sciences) and horseradish peroxidase-labeled polymer solution (Nichirei Biosciences Inc., Tokyo, Japan). Next, the sites with peroxidase were visualized with diaminobenzidine (DAB) in the presence of H_2O_2 and nickel and cobalt ions. Finally, sections were dehydrated in graded ethanol solutions, cleared in xylene, and coverslipped with a xylene-based synthetic mounting medium. Developments were monitored by light microscopy. Formalin-fixed and paraffin-embedded sections of cultured *C. albicans* (ACTT10231) and *Trichosporon asahii* (CBS2479T) were also prepared and processed in the same manner to evaluate the specificity of the probe.

ISH negative controls and PNA probes specificity test: Negative controls used for ISH consisted of omission of the probes from the hybridization reaction and slides hybridized with unlabeled probe[13].

2-2. Number of organs involved

We histologically evaluated at least 21 organs from each of 26 cases to assess the number of organs involved by candidial infection. One case was excluded from the study because the autopsy had been limited in the brain.

2-3. Distribution and morphometric analysis of CNS lesions

2-3-1. Distribution and number of lesions

To determine in detail the distribution of CNS lesions, stereographic observation was performed with a 3-dimensional (3D) reconstruction model of each case. All lesions confirmed by microscopic observation were plotted on the scheme of serial section of the CNS, and the reconstruction software (TRI-3D, RATOC Inc., Tokyo, Japan) generated 3D images indicating the number and distribution of the lesions.

2-3-2. Density and size of lesions in different areas of CNS

To determine the density and size of lesions according to anatomical region, the CNS was divided into five regions: gray and white matter of the supratentorial region, basal ganglion, brain stem, and cerebellum. The density of lesions in each region was calculated as the quotient of the total number of lesions in that region divided by mean area of each region, which had been cut for examination. The size of each lesion was also calculated using the area measured in each cross-section.

2-3-3. Distance of the lesions from the brain surface in the supratentorial region

Length was measured between the center of each lesion in the supratentorial region and the nearest point on the brain surface. The center of round or elliptical lesions was defined by the intersection of the major and minor axes. The cross-sectional area of the lesions was measured. Means and standard deviations of the distances from the brain surface were calculated and compared for lesions involving *Candida, Aspergillus, Zygomycetes*, and bacteria.

2-4. Tissue responses

Characteristics of tissue response in each case were surmised and compared by representative histological findings comprising degrees of yeast cell proliferation and infiltration of neutrophils and macrophages, which were identified by immunostaining with CD68[14].

3. Statistical analysis

The Mann-Whitney U test was used for statistical analysis. P-values < 0.05 were considered significant. Where appropriate, data are expressed as mean ± standard deviation.

Results

1. Clinical findings

The study included 19 male and 8 female patients, whose age ranged from 27 days to 89 years (52.6 ± 24.7). Solid malignant neoplasia (7 cases) was the commonest predisposing disease, followed by leukemia (5 cases), renal failure (4 cases), inflammatory liver disease (3 cases), cerebral hemorrhage (2 cases), gastric ulcer, congenital duodenal atresia, necrotizing fascitis, cardiac arrhythmia, multiple organ failure, and acute respiratory distress syndrome (1 case each). Seventeen patients (62.9%) had received a combination of antibiotics, 8 (29.6%) had received corticosteroids, and 13 (48.1%) had undergone central catheterization. There were 11 cases (40.7%) with *Candida* spp. isolated from the peripheral blood (Table 1).

2. Histopathological examination

2-1. Confirmation of *C. albicans* in paraffin-embedded tissue sections with ISH

Fungal elements present in the paraffin-embedded sections of CNS lesions from all 27 cases as well as cultured *C. albicans* showed distinct signals by ISH with the *C. albicans*-specific PNA probe. Accordingly, PNA-ISH confirmed the presence of *C. albicans* in all cases where *Candida* spp. were considered present at the time of autopsy examination. On the contrary, fungi in the sections of lesions from an autopsy of invasive trichosporonosis and of cultured *T. asahii* (controls) were negative for the PNA probe (Fig. 1).

2-2. Number of organs involved

Based on a histological review of 26 autopsy cases, after the brain, the kidney was found as the second commonest organ involved by regenerated candidiasis, followed by the lung, heart, thyroid gland, and liver (Table 2). The mean number of organs involved was